JASA ARTICLE

# North Atlantic right whale localization and source level estimation using two coherently beamformed linear arrays

Ted A. Abbot,[1,a)] Evan O. Granite,[2,b)] Vincent E. Premus,[1,c)] Eric D. Illich,[1,d)] and Aaron P. Logan[2,e)]
[1]*Ocean Acoustical Services and Instrumentation Systems, Inc., a wholly owned subsidiary of ThayerMahan, Inc., 175 Cabot Street, Suite 400, Lowell, Massachusetts 01854, USA*
[2]*ThayerMahan, Inc., 120B Leonard Drive, Groton, Connecticut 06340, USA*

**ABSTRACT:**
Two bottom-mounted, 32-channel coherently beamformed hydrophone line arrays were deployed off the coast of southern New England in March and April of 2022 in a demonstration supporting passive acoustic monitoring of marine mammals in the offshore wind construction area. On one day during that period, one or more North Atlantic right whales were detected and localized repeatedly over a two-hour period using cross-fixes measured from relative bearings to upcalls detected on both hydrophone arrays. Transmission loss (TL) testing in this region shows that the area can be characterized as a 17 log (R) environment at the 10–20 km ranges at which the whales were detected. Using the localizations and ranges to the whale(s), the received levels, and the TL, the North Atlantic right whale upcall mean source level is estimated to be 170 dB root-mean-square re 1 $\mu$Pa @ 1 m ($\sigma = 2.5$ dB) for a sample size of $n = 52$ localized upcalls.  https://doi.org/10.1121/10.0039883
(Received 27 May 2025; revised 20 October 2025; accepted 24 October 2025; published online 17 November 2025)
[Editor: Shane Guan] Pages: 3917–3928

## I. INTRODUCTION

North Atlantic right whales (NARWs) are critically endangered, with an estimated population numbering less than 400 individuals remaining (Linden, 2024). NARW calve in the winter in the waters off the southeastern coast of the United States, near Florida and Georgia, and then migrate annually to Canadian waters for the summer feeding season (Rice *et al.*, 2014). This migratory pattern means these whales transit through almost the entire eastern seaboard of the United States, including areas on the southern New England continental shelf where multiple offshore wind farms are actively being developed.

To mitigate harm to this critically endangered species during construction activity, maintenance, and operations, many monitoring and protection measures are in place, including seasonal construction restrictions, speed limits, and acoustic and visual monitoring requirements (BOEM and NOAA Fisheries, 2024). The data discussed in this paper were obtained as part of a system demonstration supporting these acoustic monitoring efforts.

Source level (SL) is one important input into performance predictions that drive acoustic monitoring requirements. The scientific literature on the average North Atlantic right whale upcall SL spans a wide range, with average SL reported as ranging from 150 to 175 dB root-mean-square (RMS) re 1 $\mu$Pa @ 1 m, as discussed in more detail in the following. It is not clear if the different results are due to differences in sensors and methodology, behavioral and regional differences, or a combination of both. Parks *et al.* (2010) also showed that individual right whales call louder in increased environmental noise, which could be another significant factor.

All discussion of vocalizations in this paper will focus exclusively on the NARW upcall vocalization. The upcall is a contact call produced by males, females, and calves (Parks *et al.*, 2011). The frequency range and duration of the upcall vary, but it is typically around 80–250 Hz, with a duration of approximately one second. In observations off the coast of southern New England (Abbot *et al.*, 2024), the upcall is both the most common and most uniquely identifiable NARW call type. Other vocalizations are outside of the scope of this paper.

Clark *et al.* (2010) reported NARW upcall SL at 172 dB RMS, $n = 100$, $\sigma = 6.6$, for samples from several bottom-mounted hydrophones deployed in Stellwagen Bank. Modeled transmission loss based on a Bellhop raytrace model was used with measured 80–250 Hz RMS received levels (RLs) to infer upcall SL. That work was extended in Clark *et al.* (2011), to arrive at a NARW upcall SL of 165 dB, $n = 353$, $\sigma = 3.5$. In the revised analysis, the RMS RLs were replaced by third octave bands centered at 160 Hz (bw = 37 Hz), and the SL was reduced by 10 log of the ratio of the bandwidth (–6.6 dB), so this result is consistent with the initial 172 dB RMS finding after adjusting for bandwidth.

Some reports are limited by sample sizes. Parks and Tyack (2005) reported SL as 150 dB RMS, for a sample size of $n = 3$ upcalls. Over half of the 160 total upcalls in their

[a)]Email: tabbot@thayermahan.com
[b)]Email: egranite@thayermahan.com
[c)]Email: vpremus@thayermahan.com
[d)]Email: eillich@thayermahan.com
[e)]Email: alogan@thayermahan.com

data set were attributed to calves, and it is not specified if the three upcalls sampled for SL inference were recorded from calves or adult whales. Similarly, Trygonis *et al.* (2013) reported SL = 155 dB RMS with a sample size of $n = 1$ upcall.

In Munger *et al.* (2011), the authors measure SL for North Pacific right whale upcalls. This is a closely related species, although North Pacific right whales are slightly larger. They find SL = 176–178 dB RMS, using the per-upcall frequency band and two different methods of localization.

In the unpublished work of Hay (2025), "Source levels of North Atlantic right whale sounds in the Bay of Fundy," the authors found 175 dB to be the lower bound SL for $n = 38$ right whale upcalls using 15 sonobuoys and a time-difference-of-arrival localization method. The analysis was conducted in the Bay of Fundy in 1999 and used KRAKENC (Porter, 1991) for transmission loss modeling. The authors note that their results may potentially be biased upwards by a natural tendency towards louder sounds being detected at longer ranges—an example of survivorship bias (Wald, 1943; Mangel and Samaniego, 1984).

This paper describes a system used to detect and localize NARWs, or "right whales," for brevity. The transmission loss environment is characterized, examples of cross-fix localizations are shown, and inferred SLs are determined. One step along this path will be the resolution of the left-right ambiguity of the array beam response via direct use of the acoustic results.

## II. METHODS

### A. Location

On March 31, 2022, at the time the right whales were first detected, two hydrophone arrays (ThayerMahan SeaPickets) (Connor and Hine, 2021; Premus *et al.*, 2022) were deployed southwest of Martha's Vineyard, MA, as shown in Fig. 1. Avon, the northern SeaPicket, was 16.1 kilometers north of the southern system Bristol. The arrays were bottom-mounted in approximately 50-meter water depth, as will be described in more detail in Sec. II B.

### B. System description

Each acoustic monitoring system is comprised of a bottom-mounted, 32-channel hydrophone array, coupled to a buoy surface expression with real-time processing and communications.

#### *1. Buoy and mooring hardware*

SeaPickets are long-endurance buoy-based acoustic detection systems designed to operate in conditions up to Sea State 6, in water depths of 15 to 75 meters, for 3- to 6-month deployments. Each SeaPicket is comprised of a 400 kg surface buoy (including ballast) made of polyethylene foam, stainless steel, and marine-grade aluminum and includes four 115 W 12 V DC solar panels and two rechargeable 12 V 200 Ah lithium iron phosphate batteries. The buoys also house the payload and control systems, and navigation lights. SeaPicket communications systems for the 2022 deployment included both cellular and Broadband Global Area Network (BGAN) modems.

The single-point mooring system uses 3 in. flex hose to both physically connect the buoy to the ocean floor anchor and to contain the data cable that transmits data between the hydrophone array and the buoy. The buoy is moored using a 1500 kg gravity anchor, which is connected to the array via 100 m of ground line and cable. Deployment begins by deploying the buoy and buoy anchor and verifying SeaPicket communications while the array remains on deck (the ground line pays out into the water as the buoy anchor is deployed). After communications are verified, the deployment ship drives off in the desired array heading direction, which may be operationally constrained by currents and weather. As the vessel moves off, the rest of the ground line pays out behind it, the array itself, and finally, the array anchor is lowered to

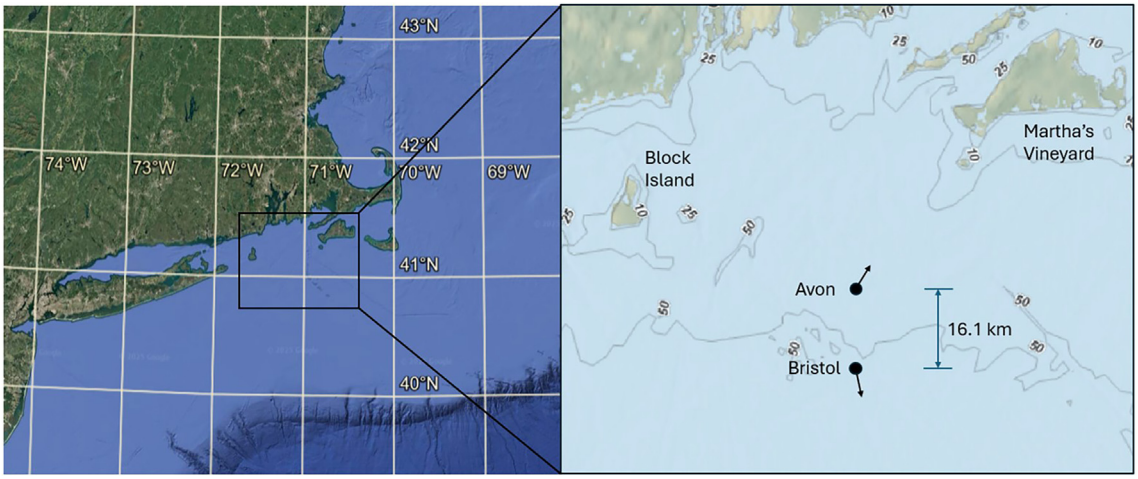


FIG. 1. Map view of deployment geometry southwest of Martha's Vineyard, with array headings as indicated by the arrows.

https://doi.org/10.1121/10.0039883

the sea floor, lifted again to apply tension, then lowered and released.

## 2. Acoustic hardware

Between the two bottom anchors, each SeaPicket fields a linear 32-channel hydrophone array manufactured by Raytheon (Portsmouth, RI). For the 2022 deployment, the arrays had a design frequency of 625 Hz with uniform half-wavelength hydrophone spacing of 1.2 meters and 37.2 m total aperture length. Hydrophone sensitivity, including pre-amp gain, was –155.6 dB re $1\ V^2/\mu Pa^2$. The hydrophone sampling rate was 2520 Hz, and data were digitized at 16-bit precision. In addition to bearing resolution, the arrays generally provide 15 dB of array gain (AG) in isotropic noise at the design frequency and approximately 10 dB of AG at the 150 Hz central frequency of the right whale upcall, two octaves down from the design frequency. The acoustic sensing payload and measured AG are described in more detail in Premus *et al.* (2022).

The acoustic digital signal processing (DSP) payload is housed in the surface buoy and both stores and processes all received acoustic data in real time. The embedded system comprises a Toradex Viola carrier board hosting a Colibri iMX7 system-on-module (Toradex, Horw, Switzerland) designed for low power consumption. The buoy and acoustic hardware are shown in Fig. 2.

## 3. Onboard software

The DSP acoustic processing architecture is a real-time, multi-stage C-language based Linux implementation that runs aboard the SeaPicket. The first stage includes data conditioning, sensor health monitoring, and fast Fourier transform (FFT) of the hydrophone time series data into the frequency domain. After the FFT, a frequency-domain conventional linear beamforming algorithm is applied, as discussed in more detail in Premus *et al.* (2022). The description that follows is an explanation of a time-domain beamformer and AG.

Beamforming is an established signal processing method (Urick, 1983) that uses synchronously sampled hydrophones to determine the direction a sound is coming from. When a planar sound wave hits a line array, it reaches each hydrophone at slightly different times, depending on the angle of incidence and the speed of sound. By analyzing these timing differences, which show up as phase shifts in the signal, the system can estimate the direction, or bearing, of the source. The entire array is coherently processed, meaning that the hydrophones are sampled synchronously. However, because the array is just a straight line, without more information, it can not be determined if the sound came from the port or starboard side. This is known as left-right ambiguity. By steering beam response in one direction at a time, from forward to aft through the full 180°, beamforming allows determination of source relative bearing, or

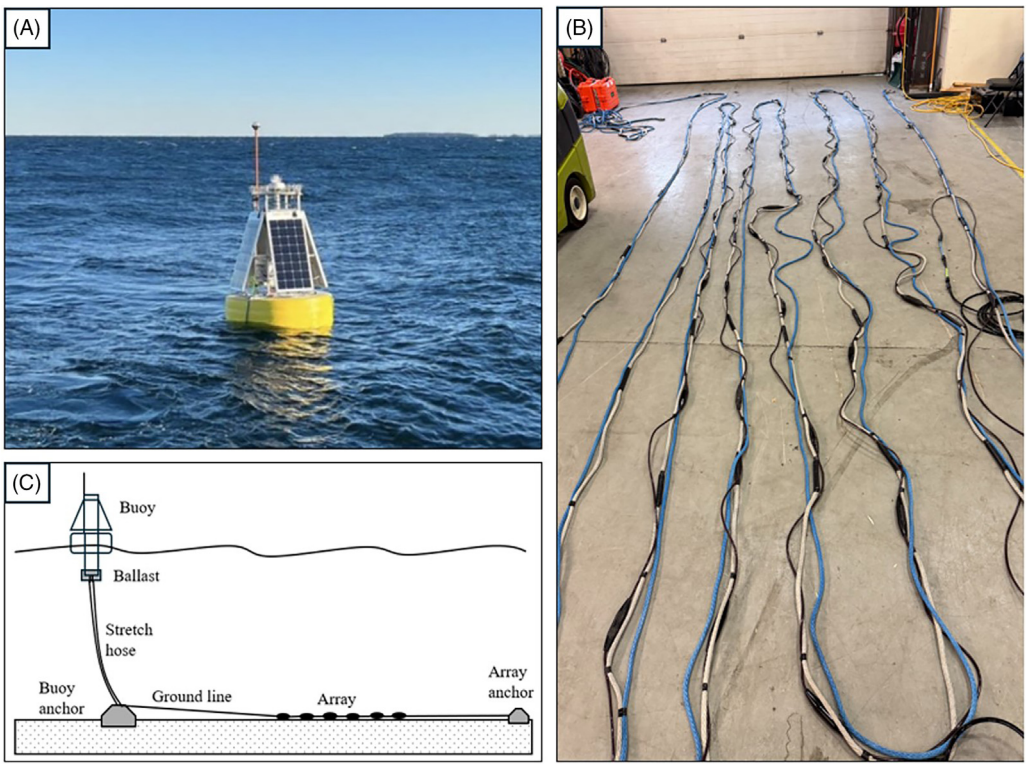


FIG. 2. A deployed SeaPicket buoy is shown in (A), while (B) is an image of a hydrophone array being prepared for deployment. The buoy is 1.5 meters in diameter, and the array is 37 meters long and deployed on the sea floor between two anchors, as shown in the simplified diagram in (C). The hydrophone array in (B) is the black cable with uniform hydrophone spacing of 1.2 meters. The array is attached to two ropes, a ground line for deployment (white) and a blue line for recovery. The black taped portions of the ground line in (B) that are not connected to the array cable are lead ballast weights, although these were not used in the 2022 deployment.

true bearings, plural (left and right), when the array heading is also known.

Beamforming also provides AG by reducing the noise from sources that are not in the direction where the beam response is steered. When the beam response is steered in a particular direction, each hydrophone's recording is delayed so that the sound lines up across the array, then summed. This makes the signal from that direction louder and clearer, while sounds from other directions, which do not line up, tend to cancel out. The result is a spatial filter that reduces the noise from other angles, and the increase in signal-to-noise-ratio (SNR) that results from this process is called AG. As a final step, sound levels are normalized back to single-hydrophone-equivalent levels to counteract the effect of summing across all 32 hydrophones.

Following conventional plane wave beamforming, a bearing-time record (BTR) is computed over the 40–510 Hz band, giving the distribution of acoustic energy over time and bearing. The BTR is sent shoreside for review, as shown in Sec. II B 4. The beamformer outputs spectrogram data along 32 beams that are uniformly spaced in relative cosine bearing. This beam spacing ensures worst-case scalloping loss (the signal loss if the arrival path is between adjacent beams) is 0.4 dB under 300 Hz. Sending the full, 32-beam spectrogram dataset shoreside in real time exceeds the available communications bandwidth capacity and, moreover, is unnecessary, so instead, a subset of seven dynamically selected interesting beams is transmitted shoreside.

All 32 beams of spectrogram data are processed through an on-board right whale classifier adapted from Abbot *et al.* (2010) and Abbot *et al.* (2012) based on the spectrogram correlation method first described by Mellinger and Clark (2000). A full treatment of the classifier is outside the scope of this paper, but to give a brief description, it was trained primarily on DCLDE 2013 data (Gillespie, 2019) and uses seven different predefined and optimized "kernels," or upcall exemplars, that each search over all beams, times, and frequencies near the expected upcall range to find upcalls. When the classifier detects vocalizations, contact reports are sent shoreside as well, which include a 6 s spectrogram snippet and the bearings.

In addition to the DSP software deployed on the buoy, a data processing and visualization architecture runs shoreside to receive, save, and display the transmitted data in near-real time. While the technical details of that architecture are outside the scope of this paper, the data visualization and mapping software will be shown in the following.

## 4. Shoreside review

Acoustic analysts in a shoreside command-and-control facility review all transmitted acoustic data in near-real time, with minor latency due to communications duty cycling. Classifier detections are overlaid on the BTR as green boxes at the estimated bearing of the source, which can be clicked on to open the detection details and associated spectrogram. An example of the interactive real-time monitoring interface is shown in Fig. 3.

The example in Fig. 3 is taken from active source testing using a J13 underwater source (Young, 1975) on September 4, 2024, in this case during the broadcasting of a real right whale upcall recording on 5 s loop. Each green box in Fig. 3 is a classifier detection and in this example the classifier can be seen to hold the signal through 16:04:51, lose contact for one minute, and then resume detections at 16:05:51. At 16:06 the classifier is still able to detect the upcalls despite the interference that remains in the source bearing, evident by the track visible on the BTR and the tonal noise present in the KMC Details spectrogram. This contact is not the source support ship, rather another unidentified ship which slowly moves out of the source bearing over the next 10 min.

In Fig. 3, all red overlaid lines on the BTR were user-selected. At each time step, only the seven most "interesting" beams are available for selection due to communications bandwidth limitations. Interesting beams are selected by an algorithm running on board the SeaPicket, and the interesting beam selection changes dynamically over time depending on what signals are present and relative RLs. With 32 beams formed, transmitting a subset of seven is typically sufficient to enable display of any signal of interest that appears on the BTR, or to track a source across beams as shown in Fig. 3. The interesting beam algorithm selects transient signals like whale vocalizations; however, it might not always include the inter-vocalization quiet periods if many other signals are present. An example to that effect can be seen in Fig. 8 of Abbot *et al.* (2024), in which humpback whales were localized during pile driving, but the BTR displayed a nearby ship track in the between-vocalization periods for one of the SeaPickets.

Note that at 16:06:16 in Fig. 3, the loud ship track is approximately 100–110 dB re 1 $\mu$Pa in a 5.9 Hz band in the central right whale upcall range of 100–200 Hz. The background noise in the right whale classifier spectrogram (KMC Details) is close to 80 dB. This indicates that AG is as high as 20–30 dB in this example. While AG is often defined assuming isotropic noise, in cases of highly directional anisotropic noise, AG may increase well beyond levels predicted by assuming isotropic noise.

## 5. Localization

Localization is performed by shoreside acoustic analysts, aided by a mapping tool connected to the real-time monitoring interface, which can plot the bearings of annotated tracks or vocalizations. After a signal is selected and annotated, the lines of bearing can be plotted on a map by using the true bearings directly from the BTR. To illustrate this, Fig. 4 shows localization accuracy against a target of opportunity, here the broadside crossing of the 200 m vehicle transport vessel *Glovis Conductor* on April 22, 2022, in a series of four snapshots as it passed Bristol.

https://doi.org/10.1121/10.0039883

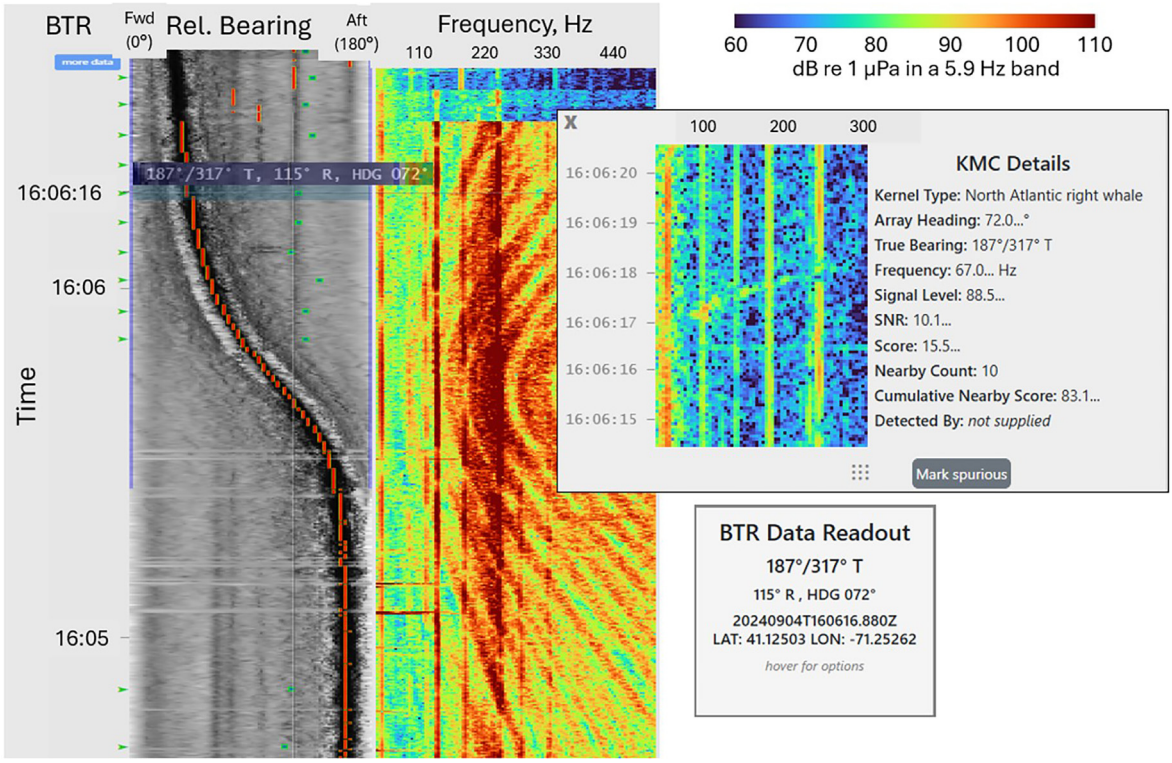


FIG. 3. The real-time monitoring interface for reviewing acoustic data, lightly edited to improve readability. This example shows almost two minutes of data, with a loud ship closest-point-of-approach (CPA) crossing from aft to forward relative bearing, with the CPA at 16:05:41 clearly identifiable from the striation patterns. During this period, calibrated active source operations transmitting NARW upcalls on a 5 s loop were being conducted at a range of 7.4 km, and the crossing interferer caused the classifier (boxes) to lose contact with the source for one minute as it approached and crossed through the same bearing as the source. On the left, the gray-scale interface is the interactive detection surface showing acoustic energy as a function of relative bearing (*X*-axis) and time (*Y*-axis) known as the BTR. Here, the crossing ship track is selected (indicated by the red overlaid line), which opens the associated spectrogram (40–510 Hz) along the track shown to the right. At the top, multiple other tracks are briefly selected to illustrate the interactive, multi-beam nature of the BTR. The spectrogram is partially covered by the Kernel Matrix Contact (KMC) "KMC details" pop-up, which was opened by clicking the detection where the mouse cursor is shown at 16:06:16. KMC and indicates that it is a classifier detection, and the KMC Details box shows that several parameters are calculated for each detection, including the bearings, signal level (RL), and SNR. The BTR Data Readout shows the true and relative bearings for the selected signal.

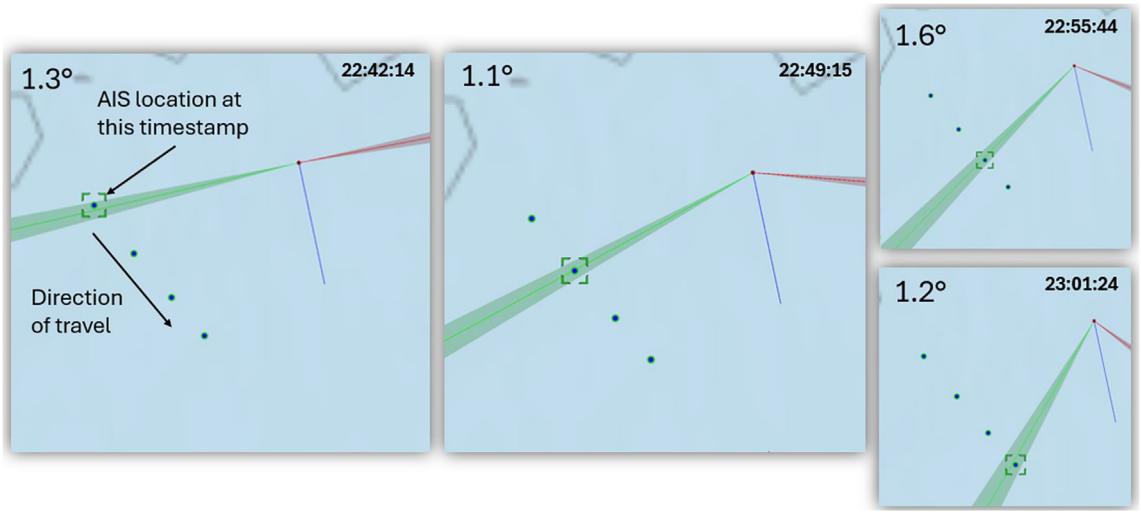


FIG. 4. Location of the ship *Glovis Conductor* via automatic identification system (AIS) data as it traveled southeast at 8.5 knots from 22:42 to 23:01 UTC. The red and green cones originate from the array, and the array orientation is indicated by the blue line. The widths of these cones are theoretical beamwidths at the array design frequency, and the red/green cones are symmetric around the array heading and represent the inherent left-right ambiguity. The ship's location and path are indicated by the series of dots from AIS records. The timestamp of each snapshot is indicated in the upper right corner, and the ship's location at that time is bracketed by the square indicator. The ship's track has been selected on the BTR (see Fig. 5) and used to plot the associated lines of bearing at the times of each AIS point. The overlaid values in the top left corner of each image indicate the bearing error of the line of bearing (at the center of the cone) relative to the bearing to the AIS ground truth at that time.

Figure 4 demonstrates the ability to track sources accurately over time and bearing. This example is a broadside crossing of a large, 200-meter length transport vessel, which was heading southeast on a course of 140° at 8.5 knots per publicly available Marine Cadastre AIS data. The broadside crossing occurred at approximately 22:42:14 UTC, while the CPA at a range of 5.6 kilometers occurred almost 10 min later at 22:51:54. Figure 5 shows the corresponding BTR and spectrogram data, with the tracks of the vessel selected and the associated spectrograms.

There were many active ships in this region at this time, as indicated by all the tracks (dark vertical lines) in the BTR in Fig. 5. However, the *Glovis Conductor* can be identified for a few reasons, including (a) this is the only vessel and track crossing broadside to Bristol at this time, and the movement across broadside is clear in the BTR; (b) the selected track contains the most acoustic energy present at this time, due to the relatively close 5.6 km range and the very large size of the vessel, and (c) the tracking agreement with AIS data already shown in Fig. 4. In the example shown in Figs. 4 and 5, bearing accuracy was continuously within 2°. Bristol was located at the coordinates 40.90074° N, 71.05913° W, and the selected tracks in Fig. 5 show the system's true bearings as 257° and 234° at the broadside crossing and the CPA, respectively. With Bristol's GPS coordinates and the public AIS data, the accuracy of this localization at broadside and the CPA is therefore independently verifiable.

Figures 4 and 5 give an example of localizing to a ship, whereas right whale upcalls are lower frequency and therefore localization accuracy is slightly reduced due to the wider beam width of the beamformer. Analysis of localization accuracy during September 2024 calibrated source operations with broadcast right whale upcalls showed an average absolute bearing error of 4.6° ($n = 1031$, $\sigma = 2.3°$), which is closer to the theoretical beamwidths of ±7° at 150 Hz at broadside. This is sufficient localization accuracy such that any error induced thereby in the inferred SL should, first, average out to zero over multiple samples, and second, in individual cases with higher error, result in less than a 1 dB impact on the inferred SL.

### C. Transmission loss (TL) and RLs

TL is often theoretically characterized by a 20 log (R) model for spherical spreading (deep water or nearby source) or as little as 10 log (R) for cylindrical spreading, which is the theoretical bound for very shallow water where all energy is constrained or ducted due to interaction with surface and bottom interfaces, if these boundaries are not lossy (Urick, 1983).

TL can be modeled and measured with active source tests, and it varies with range, frequency, and bathymetry, among other factors. TL has been studied repeatedly with calibrated active source tests in this region on the continental shelf, and results and associated detection range modeling and noise analysis were the subject of Premus *et al.* (2025). Transmission loss modeling was performed using the Navy Standard Parabolic Equation (NSPE) model, using CTD data collected during the test event and employing geoacoustic bottom parameters typical of the sediment type in the area. The most relevant transmission loss modeling and experimental results are shown in Fig. 6.

The September 2024 active source operation was conducted using a J13 underwater source, with Fig. 3 showing an example of the data on the receiving SeaPicket. The J13 is periodically calibrated at the Navy Underwater Sound Reference Division (USRD) and is monitored by a 1-meter

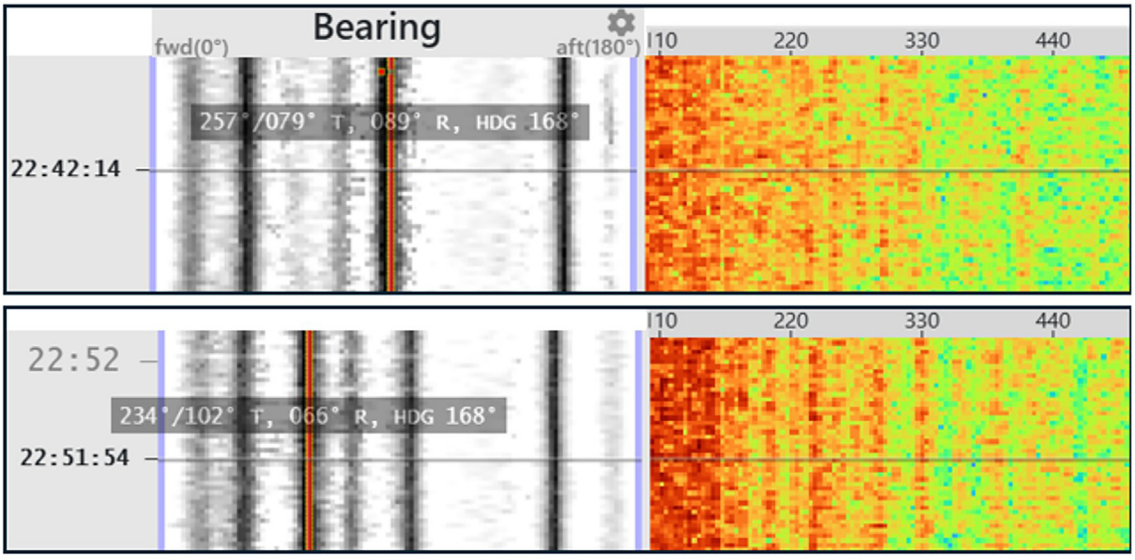


FIG. 5. Track of the ship *Glovis Conductor* at its broadside crossing at 22:42 (top) and CPA to Bristol at 22:52, 10 min later (bottom). In the upper plot, the track appears at 89° relative bearing to the array, and it is in the center of the BTR (broadside), which runs from 0 to 180° on the *X*-axis. The corresponding true bearings are 257°/79°. Over time, the track moves forward in bearing such that 10 min later at the CPA, the track now shows 66° relative bearing and 234°/102° true bearing. This corresponds to the westerly green cone moving from west-southwest to south-southwest over time in Fig. 4 as the ship passes.

https://doi.org/10.1121/10.0039883

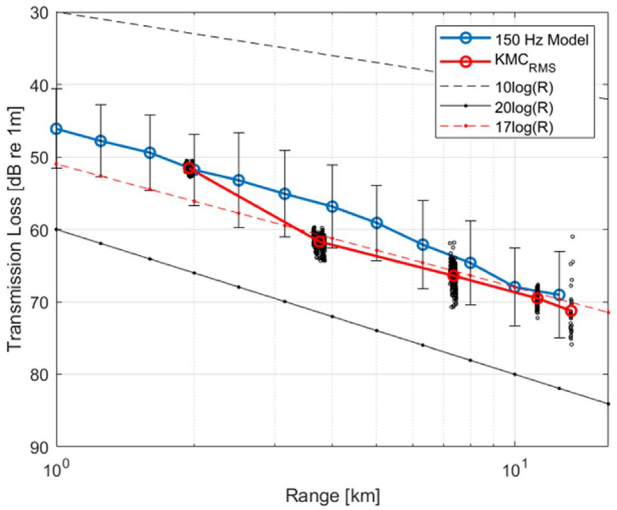


FIG. 6. The TL model (blue) vs empirically observed results from active-source testing at various ranges using a looped right whale upcall. The black points represent individual upcall detections, and the red line and red circles indicate the average measured upcall TL at each range. The 10 and 20 log (R) lines are shown, along with a 17 log (R) line indicated by the red dashed line.

reference hydrophone (calibrated internally before and after every test) to confirm the broadcast SL of 160 dB RMS. In this test, a single real upcall exemplar was broadcast on 5 s loop for an average of 30 min at each range.

RLs were calculated through the classifier in the time-frequency domain of a spectrogram, integrating over frequency and averaging over time to calculate signal power for each upcall detection. All hydrophones are calibrated, and the calculation uses the known preamp gain and hydrophone sensitivity, allowing for the calculation of RLs in absolute units (dB re 1 $\mu$Pa$^2$ in the analysis band). The calculation uses the match between the received upcall and the best-matching classifier kernel, equivalent to using the per-upcall frequency band. Testing using the 1-meter reference hydrophone data has confirmed that this method of calculating the RLs agrees to within $\pm$ 1 dB of a timeseries RMS calculation. The method of calculating RLs for transmission loss analysis shown in Fig. 6 is identical to the method used for real NARW upcalls throughout this paper.

The TL analysis in Fig. 6 shows reasonably good agreement between the modeling results and the measured TL, as measured via the broadcast upcalls, especially at longer ranges. Active source testing was also conducted in 2022 after the two arrays were, however, each deployed only at one nearby range point at 1.8 km. That test found the TL coefficient to be 16.5 at 1.8 km. This agrees with Fig. 6: TL at the 1.8 km point is somewhat more favorable than at longer ranges. Since the September 2024 test was conducted only 18 km away from the 2022 array locations, in very similar water depths, and the test covered the ranges relevant to the whales herein, the 2024 results are used to determine the TL coefficient for these ranges.

The data and modeling results in the lower right-hand corner of Fig. 6 cover the 10–20 km ranges of interest in this paper. At these ranges, the data and modeling results both agree closely with the dashed red line indicating 17 log (R). Therefore, for simplicity and ease of interpretation, 17 log (R) will be used for right whale SL inference.

## III. RESULTS

### A. Right whale cross-fix localizations

A cross-fix refers to a localization via the intersection of lines of bearing as measured on two or more SeaPickets. If such an intersection is unique or left-right ambiguity can be resolved, then the whale is localized at the "cross-fix" location of the crossing lines of bearing.

On March 31, 2022, for a period of almost two hours beginning at 01:45 UTC, a total of 52 right whale upcalls were detected and localized by Avon and Bristol. Although the systems remained deployed for a few more weeks, this brief period was the only time when definite NARW cross-fix localizations occurred. Examples are shown in Figs. 7 and 8, including the spectrograms of the upcalls as observed on each system, with spectrograms from the northern system Avon shown in the top right.

Figure 7 shows an upcall at 02:33 UTC detected on both arrays. The signal can be confirmed to be the same upcall based on review of both the spectrograms and the timestamps. There was clock drift between arrays on this deployment; hence, the fact that the call appeared to arrive at Bristol slightly before arrival at Avon is not meaningful or used in the analysis, and the timestamps shown are according to each system's respective clock. Despite the clock drift, the timestamps in conjunction with the spectrograms confirm that this is the same upcall as received on each system—note the matching duration, frequency, slope, and shape of the call in both cases.

The overlaid black boxes on each upcall are placed by the classifier based on the best classification match, while the rectangles on the side of each detection indicate the periods sampled as noise for the SNR calculation, which uses the quieter of the two noise samples and the same frequency bandwidth as the upcall. The map view shows two possible cross-fix locations at the two intersection points of the red and green cones. The center point range (W) indicates the range from each system to the western intersection point. The bearings to the intersection points are determined automatically when the vocalizations are selected and annotated on the BTR, because the BTR definitionally encodes the bearings. Another example is shown in Fig. 8.

A total of 52 upcall cross-fixes were observed over the course of two hours on March 31, 2022, from T0145-0345 UTC, where inspection of the timestamps and the upcall shapes and sizes confirms that the same upcall was detected on both systems.

### B. Resolving left-right ambiguity

In Fig. 9, another cross-fix typical of the geometry during this period is shown, displaying two ambiguous localization points, one clearly west of the two systems and one between them (referred to as the eastern location).

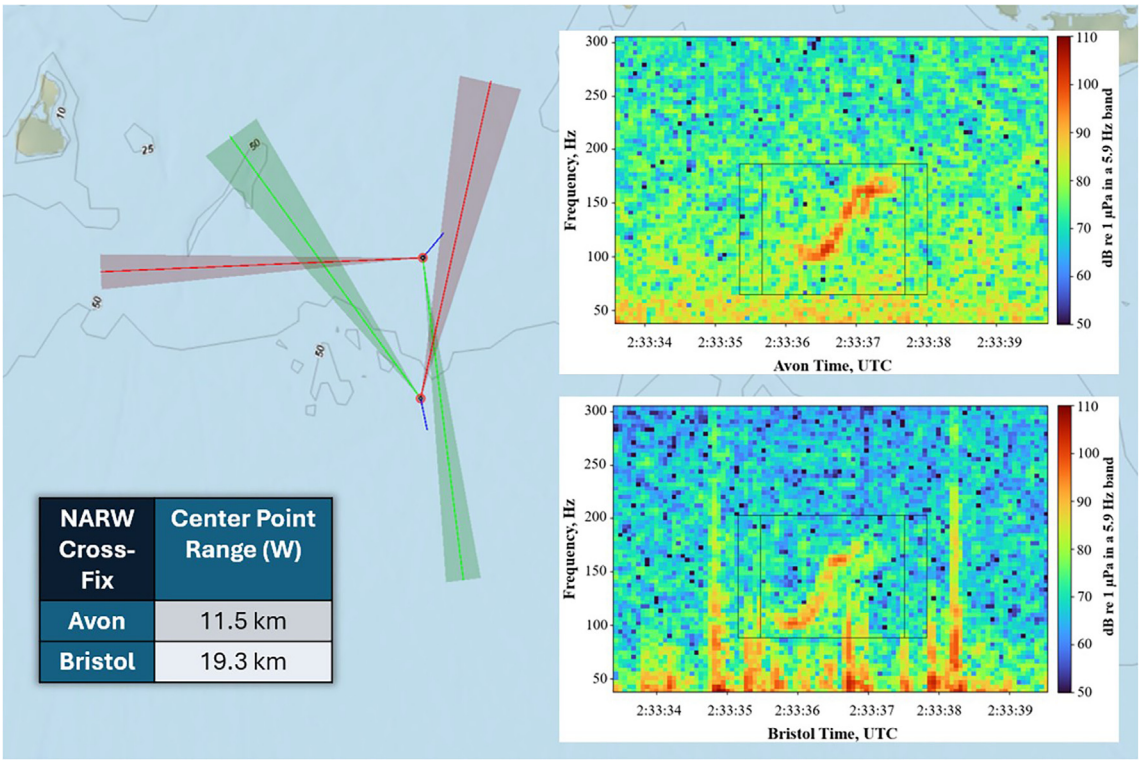


FIG. 7. Cross-fix example at 02:33 UTC. The inset spectrograms show the upcalls as received on each system, with Avon's spectrogram (the northern system) shown at the top right and the spectrogram from Bristol shown. The RLs were 103 dB on Avon and 100 dB on Bristol. The map view shows two possible bearings from each SeaPicket. Spectrogram resolution uses onboard FFT parameters with dt = 0.63 s, df = 3.94 Hz, and a Hanning window, hence, spectrogram units are reported in a 5.9 Hz band, while RL is calculated using the full upcall bandwidth on a per-upcall basis.

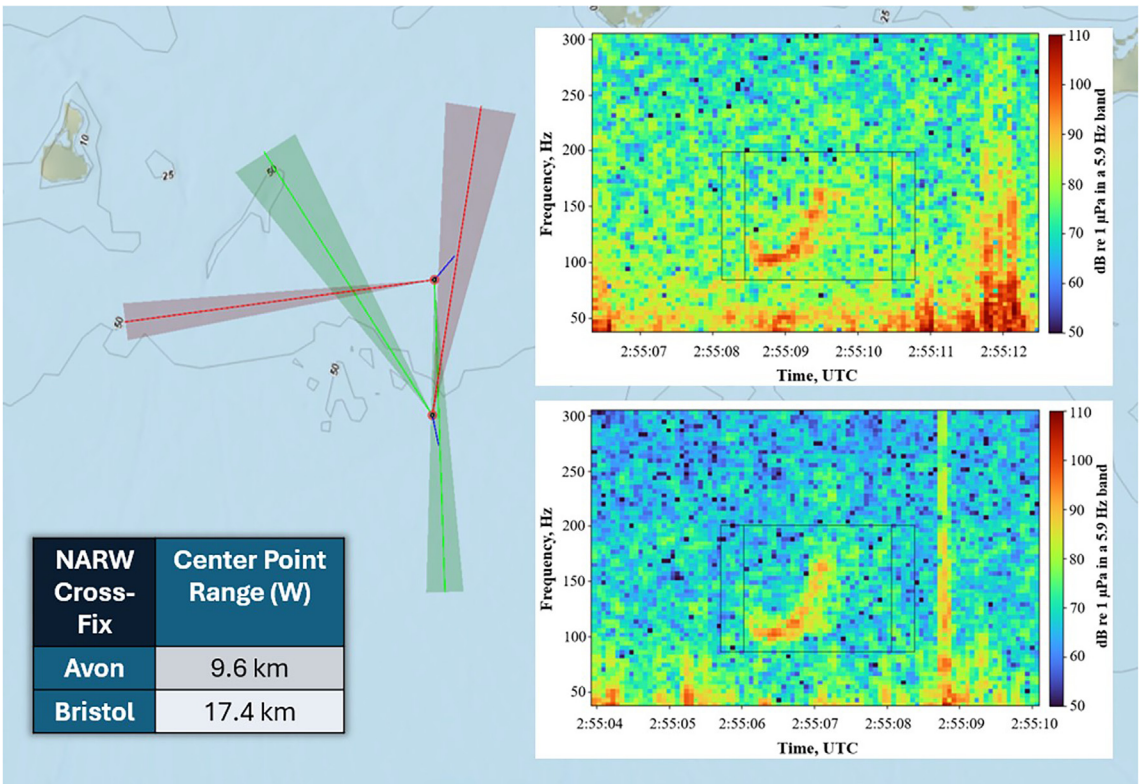


FIG. 8. Another cross-fix at 02:55 UTC. In this example, the RLs were 100 dB on Avon and 96 dB on Bristol. Timestamps indicate system time for each respective array, subject to clock drift.

https://doi.org/10.1121/10.0039883

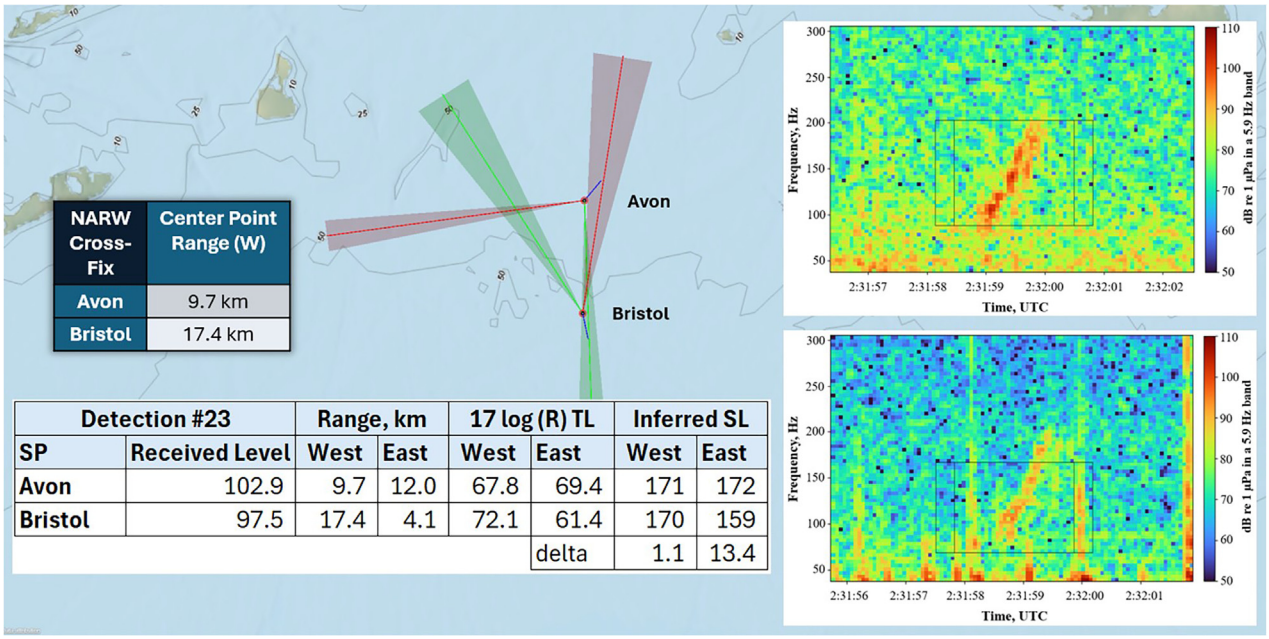


| Detection #23 | | Range, km | | 17 log (R) TL | | Inferred SL | |
|---|---|---|---|---|---|---|---|
| SP | Received Level | West | East | West | East | West | East |
| Avon | 102.9 | 9.7 | 12.0 | 67.8 | 69.4 | 171 | 172 |
| Bristol | 97.5 | 17.4 | 4.1 | 72.1 | 61.4 | 170 | 159 |
| | | | | | delta | 1.1 | 13.4 |

FIG. 9. Cross-fix example with table showing ranges, TL, and inferred SL assuming eastern and western localizations. The western location provides consistent, matching inferred SL at 170 or 171 dB, while the eastern location can be ruled out due to the >13 dB inconsistency.

Figures 7–9 use the same dynamic range, 50–110 dB re 1 $\mu$Pa in a 5.9 Hz band, to assist in visually inspecting relative signal magnitude. It can be seen from Figs. 7, 8, and 9 that the upcalls are louder when observed from Avon. This immediately suggests that the localization point should be one that is closer to Avon than to Bristol, which is only consistent with the western location.

More concretely, on a per-upcall basis, the inferred SL can be calculated assuming both the east and west locations. One given upcall can only have one SL, so if the inferred SL calculated on both systems does not match under the assumption of one of the locations, that location can be ruled out. Figure 9 shows an example of this.

The example in Fig. 9 is typical of all detections during this period. Repeating for all observations, the western localization yields an average per-upcall match between the Avon and Bristol inferred SL of 1 dB, vs an average 13 dB mismatch assuming the eastern localization. Therefore, the eastern location can be acoustically ruled out, and the whale (s) must be in the western cross-fix locations.

Using the western location, Fig. 10 shows the map view of whale localizations and the ranges from each system over time.

Figure 10 shows that the whale(s) were opening in range over time, moving slowly WNW, covering about 5 kilometers over the course of two hours. This is consistent with the relatively slow typical NARW swimming speed

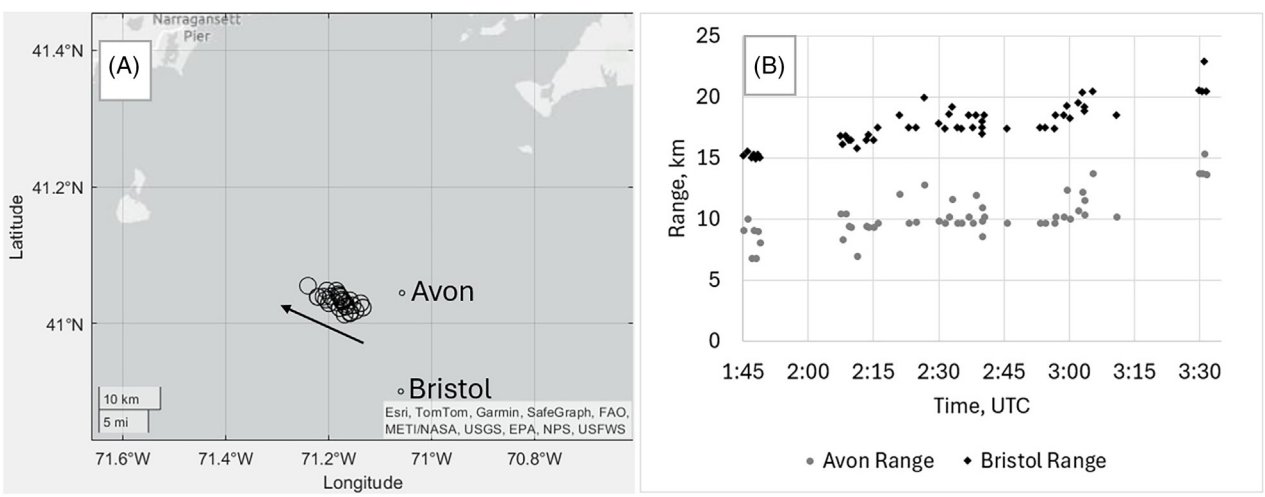


FIG. 10. A map view of whale localizations is shown in (A), with an arrow indicating the direction of travel. (B) Shows the ranges from Avon (gray) and Bristol (black) to whale localizations as a function of time.

(Hain *et al.*, 2013). The sizes of the circles in Fig. 10(A) are very approximate indicators of the areas of uncertainty (AOU) for each detection, which would normally be plotted as ovals or polygons reflecting actual beamwidths, but same-sized circles are used here for convenience. It is not known if these results are vocalizations from one whale or from a group of whales, and so it is unclear if Fig. 10 reflects bearing error to a single whale or accurate bearings to a pod of whales spread out over a few kilometers. Figure 10(B) also shows that calling bouts were interrupted by periods of silence. The periods of silence did not appear to correspond to any acoustically significant events such as passing ships.

### C. SNR and survivorship bias

SNR averaged 18 dB across all upcalls, never dropping below 10 dB. This significantly exceeds both the classifier noise recognition differential and that of the analysts reviewing the data set. This means that it is very unlikely that these results are subject to the survivorship bias (Wald, 1943; Mangel and Samaniego, 1984), which might otherwise impact a lower-SNR dataset.

Survivorship bias refers to the bias that can occur when reviewing any sample that has already passed a selection process, or "survived." This was famously first observed by Abraham Wald during World War II, who was studying the locations of bullet holes on planes that survived to return to base. Conspicuously few had bullet holes in the engines. Rather than conclude that the enemy never managed to get a shot off at the engines, he correctly deduced that the distribution of enemy fire was likely uniform, and that planes hit in the engine failed to return to base, hence the engines—and anywhere that planes seemed *not* to get hit—were in fact the areas most in need of additional armor. In the context of whales and SL, in any sample with low-SNR detections, it is probable that there are additional, quieter vocalizations that are not being detected. Using only the loudest, detected calls would result in an SL estimate biased upward by the survivorship of being detected. This was not the case here; SNR exceeded 10 dB for every upcall during this period.

### D. Inferred SLs

Inferred SLs are calculated by repeating the math shown in the inset table in Fig. 9 using 17 log (R) TL. The result is an average inferred upcall SL of 170 dB RMS ($n = 52$, $m = 93$, $\sigma = 2.5$). $N$ represents the total number of upcalls, while m is the number of array SL measurements across both systems. If the classifier detected every upcall on both systems, $m$ would equal $2n$. $M$ is slightly less than $2n$ because some upcalls were only detected through the classifier on one system and were found by an analyst on the other, which still allows for localization, but in such cases, the system-calculated RL is not available for the manually detected half of the cross-fix. The results are summarized in Fig. 11.

The average inferred SL on Bristol was 1.8 dB lower than on Avon. This analysis used the same 17 log (R) assumption for both systems, even though Bristol was farther away. It is possible that TL to the farther Bristol system is slightly underestimated by 17 log (R), leading to this difference. It is also possible that the whale(s) were closer to Avon at the start of the period than the analysis assumes, potentially due to elevated bearing error on Bristol near endfire, the direction of the array heading. However, if bearing error was a significant contributing factor, the standard deviation of inferred SL would be expected to increase for Avon, which was not observed. The standard deviations of these results are low relative to Clark *et al.* (2011), $\sigma = 3.5$, which might be due to the short period during which the whale(s) were detected. It could also support the idea that these results are all from a single whale, although this is unknown.

Of the $n = 52$ upcalls with classifier detections on at least one system, one was not detected by the classifier on Avon, and ten were not detected on Bristol. As is evident from Figs. 7, 8, and 9, the arrays were experiencing a relatively high prevalence of transient noise spikes at this time. Spring 2022 was the first SeaPicket deployment, and the arrays were ballasted to be neutrally buoyant, so the working hypothesis has been that underwater currents may have caused movement along the sea floor, generating these spikes. This has since been resolved by ballasting the arrays to lie flat and steady, and the transients have been eliminated. However, these transients are the primary reason the classifier missed some fraction of the detections. All but one of the missed detections were from Bristol, where the transient problem was more severe. An attempt to manually calculate the RLs for these upcalls was considered; however, if the upcalls were contaminated with energy from a transient spike, the data would be considered invalid, and so this step has been omitted.

Every spectrogram in this analysis has been manually reviewed, and there are no other data quality adjustments or exclusions. In a small number of cases, the RL estimate may be slightly increased by transient energy or slightly decreased by an imperfect match between the classifier and the upcall. Excluding these data points was considered, but the net impact on the average SL result was only a small fraction of a dB, and so this data quality exclusion step was omitted.

## IV. DISCUSSION

The SeaPicket system has been demonstrated to detect and localize NARWs with high localization accuracy and at ranges exceeding 20 kilometers. Beamforming allows the determination of source bearings, subject to the left-right ambiguity of a single line array. With a second array deployed, two-system cross-fix localizations allow localization and tracking of whales in near real-time. These results have also shown that left-right ambiguity can be resolved acoustically, provided that the ranges to potential localizations have

https://doi.org/10.1121/10.0039883

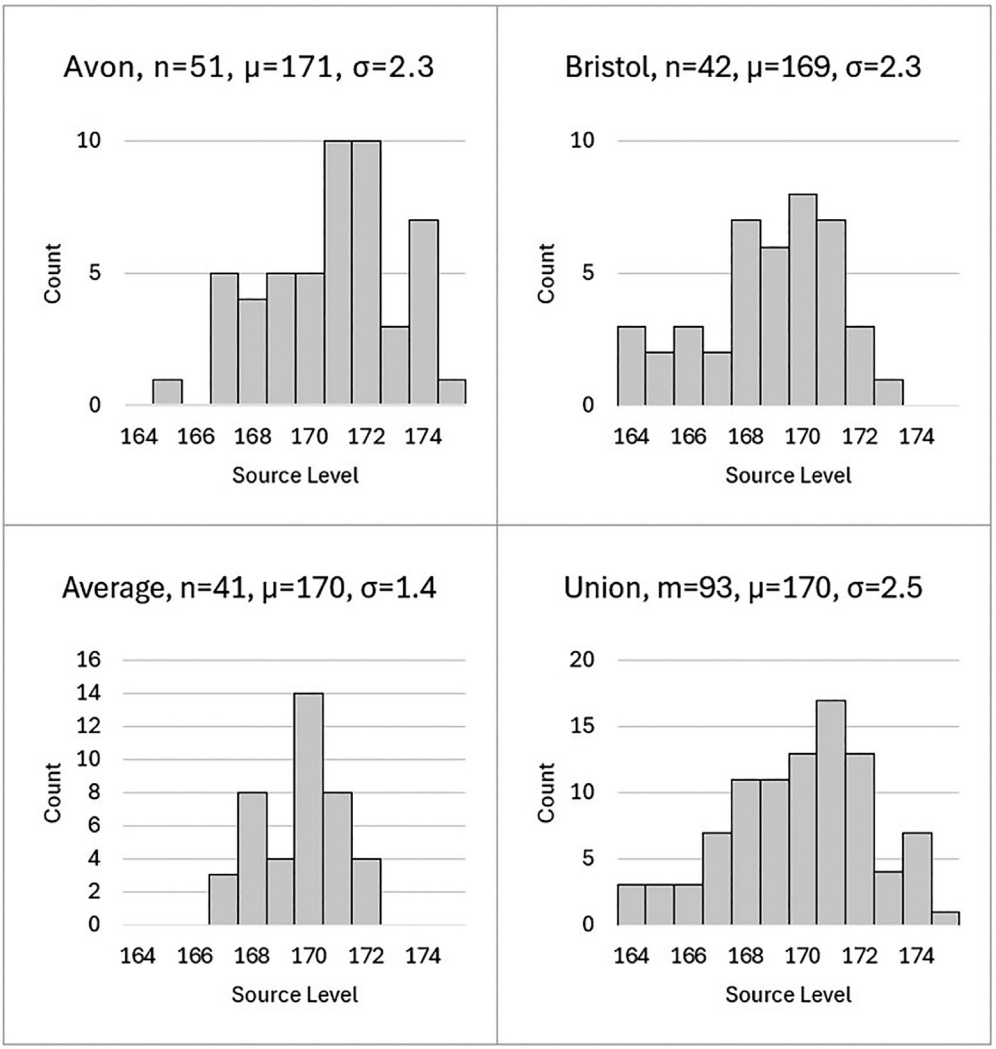


FIG. 11. Histograms of inferred SL for measurements from Avon and Bristol with sample sizes, means, and standard deviations. The Avon and Bristol results reflect the measurements from each respective system, while the Average results first average across estimated SL over both Avon and Bristol on a per-upcall basis for all upcalls where both systems had a calculated RL. The union histogram is the union of the Avon and Bristol results without averaging.

sufficient variance in range to allow this. With measured transmission loss and accurate whale locations, inferred SL can also be calculated.

Based on this analysis, the average North Atlantic right whale upcall SL is estimated to be 170 dB RMS re 1 $\mu$Pa @ 1 m ($n = 52$, $\sigma = 2.5$). The analysis uses 17 log (R) transmission loss, which has been both modeled and empirically demonstrated via calibrated source operations to be accurate for this region for the ranges in question. The results compare well with other published studies, especially after differences in TL and bandwidth assumptions are taken into consideration.

## ACKNOWLEDGEMENTS

This work would not have been possible without the efforts of dozens of individuals at ThayerMahan and OASIS, from hardware testing and integration through deployment, software, visualization, communications, and more. This work was supported by independent research and development (IR&D) investment from ThayerMahan Inc., at the direction of the CEO, VADM (Ret.) M. Connor.

## AUTHOR DECLARATIONS

### Conflict of Interest

The authors have no conflicts to disclose.

## DATA AVAILABILITY

The data that support the findings of this study are available from the corresponding author upon reasonable request.

Abbot, T., Premus, V., and Abbot, P. (**2010**). "A real-time method for autonomous passive acoustic detection-classification of humpback whales," J. Acoust. Soc. Am. **127**(5), 2894–2903.

Abbot, T., Premus, V., and Abbot, P. (**2024**). "Observations of baleen whale vocalizations in the New England offshore wind lease area from August 2023 to July 2024 using multiple high-resolution, bottom-mounted hydrophone arrays," in *Proceedings of OCEANS 2024—Halifax*, Halifax, NS, Canada (2024), pp. 1–6.

Abbot, T., Premus, V., Abbot, P., and Mayer, O. (**2012**). "Receiver operating characteristic for a spectrogram correlator-based humpback whale detector classifier," J. Acoust. Soc. Am. **132**(3), 1502–1510.

BOEM and NOAA Fisheries (**2024**). "North Atlantic right whale and offshore wind strategy," https://www.boem.gov/sites/default/files/documents/environment/BOEM_NMFS_NARW_OSW_0.pdf (Last viewed May 12, 2025).

Clark, C. W., Ellison, W. T., Hatch, L. T., and Merrick, R. L. (**2010**). "An ocean observing system for large-scale monitoring and mapping of noise throughout the Stellwagen Bank Nation Marine Sanctuary," Report to the National Oceanographic Partnership Program, Award No. N00014-07-1-1029.

Clark, C. W., Ellison, W. T., Hatch, L. T., Merrick, R. L., Van Parijs, S. M., and Wiley, D. N. (**2011**). "An ocean observing system for large-scale monitoring and mapping of noise throughout the Stellwagen Bank Nation Marine Sanctuary," September 2011 reports to the National Oceanographic Partnership Program, Award No. N00014-07-1-1029.

Connor, M., and Hine, R. (**2021**). "Continuous unmanned airborne and underwater monitoring platform," U.S. patent 11,105,662 B2.

Gillespie, D. (**2019**). "DCLDE 2013 workshop dataset," https://research-portal.st-andrews.ac.uk/en/datasets/dclde-2013-workshop-dataset (Last viewed May 12, 2025).

Hay, A. E. (2025). (private communication).

Hain, J. H. W., Hampp, J. D., McKenney, S. A., Albert, J. A., and Kenney, R. D. (**2013**). "Swim speed, behavior, and movement of North Atlantic right whales (*Eubalaena glacialis*) in coastal waters of Northeastern Florida, USA," PLoS One **8**, e54340.

Linden, D. W. (**2024**). "Population size estimation of North Atlantic right whales from 1990-2023," US Department of Commerece Northeast Fisheries Science Center Tech Memo 324 (NOAA, Washington, DC).

Mangel, M., and Samaniego, F. J. (**1984**). "Abraham Wald's work on aircraft survivability," J. Am. Stat. Assoc. **79**, 259–267.

Mellinger, D. K., and Clark, C. W. (**2000**). "Recognizing transient low-frequency whale sounds by spectrogram correlation," J. Acoust. Soc. Am. **107**, 3518–3529.

Munger, L. M., Wiggins, S. M., and Hildebrand, J. A. (**2011**). "North Pacific right whale up-call source levels and propagation distance on the southeastern Bering Sea shelf," J. Acoust. Soc. Am. **129**, 4047–4054.

Parks, S. E., Johnson, M., Nowacek, D., and Tyack, P. L. (**2010**). "North Atlantic right whales call louder in increased environmental noise," Biol. Lett. **7**, 33–35.

Parks, S. E., Searby, A., Célérier, A., Johnson, M. P., Nowacek, D. P., and Tyack, P. L. (**2011**). "Sound production behavior of individual North Atlantic right whales: Implications for passive acoustic monitoring," Endang. Species Res. **15**, 63–76.

Parks, S. E., and Tyack, P. L. (**2005**). "Sound production by North Atlantic right whales (*Eubalaena glacialis*) in surface active groups," J. Acoust. Soc. Am. **117**, 3297–3306.

Porter, M. (**1991**). "The KRAKEN normal mode program," SACLANT Memorandum SM-245 (SACLANT, Norfolk, VA).

Premus, V., Abbot, P., Illich, E., Abbot, T., Browning, J., and Kmelnitsky, V. (**2025**). "North Atlantic right whale detection range performance quantification on a bottom-mounted linear hydrophone array using a calibrated acoustic source," J. Acoust. Soc. Am. **158**, 3672–3686.

Premus, V., Abbot, P., Kmelnitsky, V., Gedney, C., and Abbot, T. (**2022**). "A wave glider-based, towed hydrophone array system for autonomous, real-time, passive acoustic marine mammal monitoring," J. Acoust. Soc. Am. **152**, 1814–1828.

Rice, A. N., Tielens, J. T., Estabrook, B. J., Muirhead, C. A., Rahaman, A., Guerra, M., and Clark, C. W. (**2014**). "Variation of ocean acoustic environments along the western North Atlantic coast: A case study in context of the right whale migration route," Ecol. Inform. **21**, 89–99.

Trygonis, V., Gerstein, E., Moir, J., and McCulloch, S. (**2013**). "Vocalization characteristics of North Atlantic right whale surface active groups in the calving habitat, southeastern United States," J. Acoust. Soc. Am. **134**, 4518–4531.

Urick, R. (**1983**). *Principles of Underwater Sound* (McGraw-Hill, New York).

Wald, A. (**1943**). *A Method of Estimating Plane Vulnerability Based on Damage of Survivors* (Statistical Research Group, Columbia University, New York).

Young, A. M. (**1975**). "An underwater acoustic source for the infrasonic and low-audio-frequency range (USRD type J13 transducer)," Underwater Sound Reference Division (Naval Research Laboratory, Washington, DC).